The Agadir Slide offshore NW Africa: Morphology, emplacement dynamics, and potential contributions to the Moroccan Turbidite System

Wei Li[a,b,*], Sebastian Krastel[b], Tiago M. Alves[c], Morelia Urlaub[d], Lisa Mehringer[e], Anke Schürer[e], Peter Feldens[f], Felix Gross[b], Christopher J. Stevenson[g], Russell B. Wynn[h]

[a] Key Laboratory of Ocean and Marginal Sea Geology, South China Sea Institute of Oceanology, Chinese Academy of Sciences, 510301 Guangzhou, P.R. China

[b] Christian-Albrechts-Universität zu Kiel, Institute of Geosciences, Otto-Hahn-Platz 1, 24118 Kiel, Germany

[c] 3D Seismic Lab. School of Earth and Ocean Sciences, Cardiff University, Main Building, Park Place, Cardiff, CF10 3AT, United Kingdom

[d] GEOMAR Helmholtz Centre for Ocean Research Kiel, Wischhofstr. 1-3, 24148 Kiel, Germany

[e] Faculty of Geosciences and MARUM, Center for Marine Environmental Sciences, University of Bremen, Klagenfurter Straße, 28359 Bremen, Germany

[f] Leibniz Institute for Baltic Sea Research, Warnemünde, 18119 Rostock, Germany

[g] School of Earth, Ocean and Ecological Sciences, University of Liverpool, Liverpool L69 3GP, United Kingdom

[h] National Oceanography Centre, European Way, Southampton, Hampshire SO14 3ZH, United Kingdom

*Correspondence to: Dr. Wei Li (wli@scsio.ac.cn)

Abstract

A newly identified large-scale submarine landslide on the NW African margin (Agadir Slide) is investigated in terms of its morphology, internal architecture, timing, and emplacement processes using high-resolution multibeam bathymetry data, 2D seismic profiles, and gravity cores. The Agadir Slide is located south of the Agadir Canyon at a water depth ranging from 500–3,500 m, with an estimated affected area of approximately 5,500 km^2. The analysis of the Agadir Slide's complex morphology reveals the presence of two headwall areas and two slide fairways (the Western and Central slide fairways). The volume calculations indicate that approximately 340 km^3 of sediment accumulated downslope along the slide fairways (approximately 270 km^3) and Agadir Canyon (approximately 70 km^3). Novel stratigraphic correlations based on five gravity cores indicate an emplacement age of approximately 142 ± 1 ka for the Agadir Slide. However, the emplacement dynamics suggest that the Agadir Slide developed in two distinct, successive stages. The presence of two weak layers (glide planes) is a major preconditioning factor for the occurrence of slope instability in the study area, and it is likely local seismicity related to fault activity and halokinesis triggered the Agadir Slide. Importantly, the Agadir Slide neither disintegrated into sediment blocks nor was it transformed into turbidity currents. The emplacement timing of the Agadir Slide does not correlate with any turbidites that have been recorded downslope across the Moroccan Turbidite System.

Keywords: Agadir submarine slide; Turbidity current; Multibeam bathymetry; Moroccan Turbidite System; Northwest Africa.

1. Introduction

Submarine landslides are ubiquitous across continental margins (Hampton et al., 1996; Masson et al., 2006; Krastel et al., 2014). They are one of the key mechanisms that transport sediment from continental shelf and upper slope areas into deep-sea basins (Masson et al., 2006). Submarine landslides are capable of generating damaging tsunamis that affect both local and distal coastal communities and associated infrastructure (Mosher et al., 2010; Tappin et al., 2014). On a local scale, large-volume and fast-moving submarine landslides disintegrate to produce turbidity currents through mixing processes with the surrounding sea water (Talling et al., 2007a; Clare et al., 2014). Turbidity currents are more mobile than their parent landslides and are capable of transporting sediment over thousands of kilometers to reach the distal Abyssal Plains (Talling et al., 2007b; Wynn et al., 2010;

Stevenson et al., 2014). For geohazard assessments, it is important to understand why some landslides form turbidity currents while others do not, since turbidity currents can travel at relatively high speeds (tens of m/s) and pose a major geohazard to sea floor infrastructure such as telecommunication cables and pipelines (Piper et al., 1999).

The Moroccan Turbidite System extends 1,500 km from the head of the Agadir Canyon to the Madeira Abyssal Plain (Fig. 1), and it has hosted some of the largest (with volumes exceeding 150 km^3) landslide-triggered turbidity currents that have occurred in the past 200 ka (Wynn et al., 2002; Talling et al., 2007a; Frenz et al., 2009; Wynn et al., 2010; Stevenson et al., 2014). The Moroccan Turbidite System fills three interconnected sub-basins: the Seine Abyssal Plain, the Agadir Basin, and the Madeira Abyssal Plain (Wynn et al., 2002; Fig. 1). Previous studies have developed a robust geochemical and chronostratigraphic framework across the Moroccan Turbidite System, allowing the correlation of individual turbidite beds across the continental margin (Wynn et al., 2002; Frenz et al., 2009; Hunt et al., 2013a). The turbidites originate from three areas (Fig. 1): (1) organic-rich siliciclastic flows sourced from the Moroccan margin, which are fed into the system via the Agadir Canyon and several submarine canyons (Wynn et al. 2002; Frenz et al., 2009; Hunt et al., 2013a), (2) volcaniclastic flows sourced from either the Canary Islands or Madeira (Hunt et al., 2013b), and (3) carbonate-rich flows sourced from local seamounts (Wynn et al., 2002). The first group represents the largest deposits, and due to their large volumes, their sources are most likely submarine landslides originating from the upper regions of the Moroccan continental slope (Talling et al. 2007a). However, to date, no major landslide scars have been documented in the upper regions of this system.

The study area is situated on the Moroccan continental margin at water depths ranging from 30 to more than 4,000 m (Fig. 1). Recently, a large-scale submarine landslide (Agadir Slide) was identified in this area based on hydroacoustic data (Fig. 2; Krastel et al., 2016). However, several questions on the Agadir Slide must still be addressed, such as (i) how the Agadir Slide was emplaced and (ii) whether the Agadir Slide was a source landslide for turbidites in the Moroccan Turbidite System. In this contribution, we combine high-resolution multibeam bathymetry, 2D seismic profiles, and gravity cores with the objectives of: a) investigating, in detail the seafloor morphology of the Agadir Slide, b) describing the internal architecture of the Agadir Slide and estimating its volume, c) determining the timing of the Agadir Slide, and d) discussing the emplacement processes and flow behavior of the Agadir Slide.

2. Geological setting

2.1. The Northwest African margin

The northwest (NW) African margin is characterized by a flat continental shelf, generally 40–60 km wide, and a shelf break at a water depth of 100–200 m (Seibold, 1982; Hühnerbach and Masson, 2004). The continental slope has a width of 50–250 km beyond the shelf break with a slope gradient of 1–6° (Fig. 1; Dunlap et al., 2010). The continental slope continues into the continental rise at water depths of 1,500–4,000 m, with gradients ranging from about 1° on the lower slope/upper rise to 0.1° on the lower rise (Seibold, 1982). The continental rise is generally 100–150 km wide and terminates at water depths of 4,500–5,400 m, beyond which the flat expanse of the Agadir Basin, the Seine Abyssal, and the Madeira Abyssal Plains occur (Fig. 1).

The NW African margin is dissected by numerous canyons and channels, and is interrupted by multiple volcanic islands and seamounts, which creates a topographically complex setting that greatly influences local sedimentary processes (Wynn et al., 2000). Prominent bathymetric features near the study area include a group of volcanic seamounts to the west and the Canary Islands to the southwest (Fig. 1). The Agadir Canyon extends from the edge of the shelf break and extends to the upper continental rise, opening onto the Agadir Basin (Wynn et al., 2000; Krastel et al., 2016) (Fig. 1).

The Moroccan margin has experienced multiple deformation episodes associated with toe-thrust anticlines during the Cretaceous and the Cenozoic (Tari and Jabour, 2013). Renewed uplift and neotectonic inversion of the Atlas Mountains, which tilts the margin toward deeper water, causes the continual deformation of salt structures (Tari and Jabour, 2013). The NW African continental margin has been a region of slope instability throughout the Quaternary due to tectonic movements, and some of the world's largest submarine landslides have occurred in this region over the past 200 ka (Krastel et al., 2012).

2.2. The Moroccan Turbidite System

With a total length of 1,500 km, the Moroccan Turbidite System on the northwest African continental margin is one of the longest turbidite systems in the world (Fig. 1; Wynn et al., 2002). The morphology of the Moroccan Turbidite System is largely controlled by the position of volcanic islands, seamounts, and salt diapirs (Wynn et al., 2000). The Moroccan Turbidite System extends along three interlinked deep-water basins: the Agadir Basin, the Seine Abyssal Plain, and the Madeira Abyssal Plain (Wynn et al., 2002).

The Moroccan Turbidite System is characterized by a relatively low turbidite frequency of approximately 1 event every 15,000 years (Wynn et al., 2002), where the turbidite beds are separated by discrete hemipelagic intervals (Frenz et al., 2009; Hunt et al., 2013a). Previous studies have identified 14 turbidite beds (AB1 to AB14) in the Moroccan Turbidite System spanning the past 200 ka (Wynn et al. 2002; Talling et al. 2007a; Hunt et al. 2013a). The majority of these turbidites derive from the Moroccan margin, including AB3 and AB4 during Marine Isotope Stage (MIS) 3, AB5 at approximately 60 ka, AB 6 during the MIS 4/5, and AB7, AB 9, and AB11–AB13 during MIS 5 (Wynn et al., 2002; Frenz et al., 2009).

Turbidite AB12 is the largest turbidite in the Moroccan Turbidite System and contains approximately 230 km^3 of sediment (Frenz et al., 2009). Frenz et al. (2009) suggested that AB1 (approximately 1 ka; Thomson and Weaver, 1994) derives from the continental margin south of the Canary Islands and is related to the recent re-activation of the Sahara Slide. Turbidite AB2 (approximately 15 ka) is volcanoclastic and is likely sourced from the El Golfo landslide that surrounds the western Canary Islands (Frenz et al., 2009). Turbidite AB8 (during MIS 5) originates from a relatively localized failure of presorted volcaniclastic sand that derives from the flanks of the Madeira (Frenz et al., 2009; Hunt et al., 2013a). AB10 (during the MIS 5) occurs throughout the

Agadir Basin except along the northern margin and the mouth of the Agadir Canyon (Frenz et al., 2009). Previous studies have suggested that Turbidite AB 14 was deposited at approximately 160 ka and likely derives from the Icod landslide on the northeast flank of Tenerife.

3. Data and methods

The data set used in this study was collected offshore of northwest Morocco during the Maria S. Merian research cruise MSM32 in October 2013. The dataset comprises multibeam bathymetry data, 2D seismic profiles, and gravity cores (Figs. 2 and 3).

3.1. Multibeam bathymetry data

During the MSM32 cruise, a hull-mounted Kongsberg Simrad system (EM122) was used to accurately map the bathymetry. The EM122 system operates at a nominal frequency of 12 kHz, an angular coverage sector of up to 150°, and 864 soundings per ping. The multibeam bathymetric data covers approximately 13,000 km^2 from the Agadir Slide headwall area, at a water depth of 600 m, extending to the Agadir Canyon at a water depth of 4,500 m (Fig. 2). The QPS FLEDERMAUS and MBSYSTEM software was used to process the multibeam data. During the data processing, we made frequent, general quality checks (navigation, attitude data, and sound velocity profiles), we generated a CUBE surface, and removed spikes, especially where individual profiles overlapped. The processed bathymetric data were gridded for visualization and subsequent volume calculations. Bathymetric data grids of 30 by 30 m were generated and geographically placed relative to the WGS84 ellipsoid.

Minimum-curvature splines in the tension interpolation were used to generate the pre-slide topography at a later stage (Smith and Wessel, 1990). The estimated volumes of evacuated sediment in the Agadir headwall area and the Central slide fairway were calculated by subtracting the interpolated surface from the seafloor topography (Fig. 2).

3.2. 2D seismic data

An 88-channel, 137.5 m-long Geometrics GeoEel streamer and a standard GI-gun (1.7 L primary volume) were used to acquire high-resolution multichannel seismic data. Fifty-six two-dimensional (2D), high-resolution multichannel seismic profiles, with a total length of approximately 1,500 km, were acquired during the MSM32 cruise. For the signal processing, we used the VISTA® 2D/3D Seismic Data Processing Software. The basic processing steps included trace binning at 12.5 m, filtering, gain recovery with increasing depth, NMO-correction, stacking, and post-stack finite-difference migration. The IHS Kingdom® software was used to visualize and interpret the seismic data. The top and bottom surfaces of the Agadir Slide were interpreted along all the seismic lines and were gridded by using the minimum-curvature gridding algorithm (Smith and Wessel, 1990). The accumulation volumes of the Agadir Slide deposits in the Central and Western slide fairway and the Agadir Canyon were estimated by subtracting the grids created from the top and bottom surfaces of the Agadir Slide. We used a seismic velocity of 1650 m/s for the time-depth conversion.

3.3. Gravity cores

Three gravity cores (MSM32-8-2, MSM32-28-1, and MSM32-14-1), up to 10 m in length, were recovered from the Agadir Slide area (Fig. 3). In addition, we examined two other gravity cores (GeoB 2415-2 and GeoB4216-1) located in the immediate vicinity of the Agadir Slide (Fig. 3). These cores were collected during the RV METEOR cruise 37/38 in 1997 (Wefer et al., 1997). A handheld Magnetic Susceptibility Meter SM 30 from ZH Instruments was used to measure Magnetic Susceptibility in 2 cm-intervals. Magnetic Susceptibility measurements on cores GeoB 4215-2 and GeoB 4216-1 are taken from Kuhlmann et al. (2004) and Freudenthal et al. (2002), respectively. All the cores were correlated across the study area to understand the stratigraphic framework of the Agadir Slide. We used the down core magnetic susceptibility profiles, distinct sediment color changes, sedimentary properties, and key sedimentary structures to construct a correlation framework. Age models for the GeoB already exist (Freudenthal et al., 2002; Kuhlmann et al., 2004) and were extrapolated to the MSM32 cores, which provided an age model for Agadir Slide emplacement.

4. Results

4.1. Morphology of the Agadir Slide

The Agadir Slide extends from a water depth of 500–3,500 m and traverses a total length of 350 km, which corresponds to an area of approximately 5,000 km^2 (Fig. 2). The Agadir Slide is located approximately 200 km south of the Agadir Canyon. A prominent sidewall cut into the continental slope borders the Agadir Canyon to the south (Figs. 2 and 3a). The Agadir Slide is divided into four domains: (i) the upper headwall area, (ii) the lower headwall area, (iii) the Western slide fairway, and (iv) the Central slide fairway (Fig. 3a and b). In addition, five seamounts, denoted SM 1 to 5, occur on the seafloor, affecting the morphology of the Agadir Slide (Fig. 3a). The term fairway, used in this study, refers to the debris flow pathway, clearly visible on the bathymetric map (Krastel et al., 2016).

The upper headwall area is located at a depth of 500–1,600 m (Fig. 3a). The width of the headwall area is approximately 2 km in the upper region and gradually increases to approximately 35 km downslope, characterizing the headwall area by an overall V-shape in plain view (Fig. 3a). It has a length of 40 km and covers an area of approximately 560 km^2. The height of the headwall scarp in domain (i) is approximately 125 m (Fig. 4a). The slope gradient within the headwall area varies between 0.6 and 4° (Fig. 3b). Seafloor morphology within the headwall area is smooth and slide blocks are not easily recognized. In contrast, several submarine canyons and a field of sediment waves developed upslope of the upper headwall area in the Agadir Slide (Fig. 4a). The sidewall scarp at the eastern border of the upper headwall area is approximately 35 km in length and has an N-S orientation. The western sidewall scarp has a length of approximately 40 km and its orientation changes from NNW to NW at a depth of 1,250 m. Both sidewall scarps have a height of up to 90 m and disappear gradually downslope (Figs. 3a and 4a). Several (minor) slide scars have been identified near the upper headwall area and in the northwestern corner of the Central slide fairway (Figs. 3a and b).

The lower headwall area is located at depths from 1,800 to 1,950 m and it has a width of approximately 9 km (Fig. 4b). The sidewall scarps of the lower headwall area are bordered by SM 3 to the west and by SM 4 to the southwest. The headwall scarp in the lower headwall area has a height of approximately 100 m (Fig. 4b).

We consider the Western slide fairway as a northwest continuation of the Agadir Slide headwall at a depth of approximately 1,750 m (Figs. 3a and b). The Western slide fairway is bounded by the SM 1 and SM 2 to the south, and by the western sidewall scarp of the Central slide fairway to the east. Its western border is characterized by the formation of positive relief when compared with the adjacent seafloor (Fig. 2a). The Western slide fairway spans an area of 1,250 km^2 and has a length of approximately 65 km. The width of the Western slide fairway increases downslope to a maximum value of 30 km at a depth of 1,950 m and then gradually decreases (Fig. 3a), and afterward decreases gradually downslope (Fig. 3a). The regional slope gradient within the Western slide fairway also decreases from 0.6 to 0.2° downslope (Fig. 3b). The seafloor surface is smooth with only one pronounced incision surface (at a depth of approximately 20 m) near the headwall area (Fig. 3a). The western boundary of the Western slide fairway is characterized by nine meters of positive relief compared with the nearby undeformed seafloor (Fig. 4c).

The Central slide fairway connects the Agadir Slide headwall area with the Agadir Canyon; it is the major pathway for slide deposits traveling into the canyon (Fig. 3a and b). We observe distinctive sidewall scarps in the northern and southern regions of the Central slide fairway, with heights ranging from 30 to 50 m. In the middle region, scarp orientation changes from N–S to NE–SW and seafloor morphology transforms from distinctive sidewall scarps into a series of positive relief features (approximately 15 m) at depths of 2,100–2,200 m (Figs. 3a and 4d). Further to the north, the Central slide fairway enters the Agadir Canyon exhibiting a marked change in the slope gradient from 0.5 to 1.8°, at a depth of 2,500 m (Figs. 3b and 7b). In addition, we have identified a pronounced NW-trending slide scarp in the eastern region of the Central slide fairway (Fig. 3a).

4.2. Internal architecture of the Agadir Slide

The internal seismic character of deposits in the Agadir Slide are characterized by a highly disrupted to chaotic and transparent seismic facies, and are bounded above, below, and laterally by continuous strata (Figs. 5, 6, and 7). Sediments above the mass-transport deposits, generated by the Agadir Slide, have a nearly consistent thickness for all the seismic profiles (Figs. 5, 6, and 7). We have identified two basal shear surfaces (BSS I and BSS II), and each form a continuous plane that dips parallel to the underlying strata (Figs. 5b, 6a, b, and c). These basal shear surfaces are located at different stratigraphic depths, where BSS II is deeper than BSS I (Figs. 6a and b). There are erosional remnants on the downslope side of SM 3 and the western boundary of the Central slide fairway, which seem to separate BSS I and BSS II (Figs. 6a and b). The BSS I extends from the upper headwall area to the Western slide fairway (Figs. 3b and 4c), while BSS II only exists, upon observation, in the Central slide fairway (Figs. 3b, 5b, and c).

The deposit thickness in the Agadir Slide in the upper headwall area is quite thin compared with deposit thickness in the Western and Central slide fairway. Numerous faults are visible on the crests of the salt domes (Figs. 6b and c). Several faults propagated vertically and terminated along the basal shear surfaces of the Agadir Slide. Several salt diapirs affect the deposits in the Agadir Slide (Figs. 5b, c, and 6b). In several areas, slide deposits appear to be elevated by the salt diapir, which may indicate salt diapir activation during or after the Agadir Slide occurred (Fig. 5b). The toe region of the Central slide fairway contains multiple small-scale faults (Fig. 6c). Based on the seismic line direction, the orientations of these faults are roughly parallel to the sliding direction in plain view. On the eastern flank of the Central slide fairway, accumulations of slide material are higher than the surrounding unaffected sea floor, which forms a marked positive relief above the original sea bed (Figs. 6c, d, and 7a).

4.3. Volume estimates

Evacuated material: We have reconstructed the pre-slide bathymetry within the Agadir Slide headwall area and the Central slide fairway to estimate the total evacuated volume (Figs. 8a and b). A total sediment volume of approximately 36 km^3 was evacuated from the Agadir Slide headwall area, which affected a larger area of approximately 560 km^2 (Fig. 8a). This volume and area indicate that the removed sediment had an average thickness of 65 m. Strata evacuated from the Central slide fairway has a volume of 135 km^3 and a mean height of 50 m (Fig. 8b). At the western and eastern border of the Central slide fairway 0.4 km^3 of slide deposits, with a mean height of 5 m, have accumulated above the pre-slide topography.

Deposited material: We estimate the deposit volume in the Agadir Slide in the Central and Western slide fairway and the Agadir Canyon based on the interpreted seismic data (Figs. 8c, d, and e). In the headwall area, slide deposit thickness is quite small (<25 m), which indicates that erosion prevails over deposition (Fig. 5a). Deposits in the Agadir Slide have a volume of 63 km^3 in the Western slide fairway, affecting an area of 1,240 km^2 (Fig. 8c). The average slide deposit thickness in this area is 51 m. In the Western slide fairway, the majority of the mobilized sediment was deposited near the western flank and in the southern region, where the slide deposit thickness reaches 110 m (Fig. 8c). In the Central slide fairway, an accumulated total of 206 km^3 of Agadir Slide deposits cover an area of 2970 km^2 with a mean thickness of 70 m (Fig. 8d). Most Agadir Slide deposits are distributed throughout the eastern region of the Central slide fairway (Fig. 8d). The volume and area affected by the slide deposits within the Agadir Canyon are 68 km^3 and 1686 km^2, respectively. Agadir Slide deposit thickness in the canyon varies greatly with an average thickness of 40 m. At the southern end, thicknesses are less than 30 m increasing to 40 m further north. The largest slide deposit accumulation occurs at the northern border of the central part of the Agadir Canyon.

In summary, a total sediment volume of 170 km^3 was evacuated, while 340 km^3 of sediments were deposited by the Agadir Slide.

4.4. Age model for the Agadir Slide

We divided the sediment sampled in the gravity cores into two units, i.e., Units A and B, based on visual descriptions of the cores (Figs. 9a and b). Unit A, which forms the upper part of the sediment cores, contains muddy, carbonate-rich, nannofossil ooze in various nuances of light brown, red, and green (Fig. 9a). Unit A is a continuous succession of hemipelagic sediment comprised of fine-grained biogenic and terrigenous material. Unit B is located in the lower part of the sediment cores and underlies Unit A (Fig. 9a). Sediment in Unit B is light beige, brown, red, and green and contains foraminifera-bearing, carbonate-rich, nannofossil ooze (Fig. 9a). Slump folds and internal shearing have deformed Unit B and, therefore, we interpret Unit B as the Agadir Slide deposits.

Core GeoB4216 is located to the west of the study area in a region unaffected by the Agadir Slide (Figs. 3a and 9b). The grain size ranges from silty mud to muddy fine-sand and layers are characterized by varying colors. Based on these observations, we suggest that the entire core corresponds to the characteristics of Unit A.

Magnetic Susceptibility was measured in Unit A to correlate sediment-core data across the study area and to establish stratigraphic relationships (Fig. 9b). Magnetic Susceptibility was not measured in Unit B due to the presence of remobilized strata. Magnetic Susceptibility profiles in all cores show distinct tie-points, which correlate across the study area despite the fact that only relative values were measured for the MSM32 cores (Fig. 9b). Magnetic susceptibility correlation allowed the extrapolation of the GeoB core age model (Kuhlmann et al., 2004; Freudenthal et al., 2002) to the MSM32 cores. The MSM32 cores have relatively constant sedimentation rates of 4.4, 4.0, and 4.1 cm/ka for cores MSM32-8, 28, and 14, respectively. The oldest Magnetic Susceptibility tie-point occurs between 5 and 12 cm above the Agadir Slide deposits and dates to 140 ka. Assuming a similar sedimentation rate below this 140 ka horizon, we estimate an age of 142 ± 1 ka for the emplacement of the Agadir Slide.

5. Discussion

5.1. Emplacement processes of the Agadir Slide

The morphological features and internal architecture of the Agadir Slide, when combined with our age constraints, provide important evidences on the emplacement of the Agadir Slide. The Agadir Slide did not affect the present-day seafloor and is draped by recent sediments (Figs. 5b and 9a). Gravity core dating in the study area provides an age of 142 ± 1 ka for the main slide body (Fig. 9b). Agadir Slide bathymetric data and seismic profiles illustrate that two headwall areas exist (the upper and lower headwall areas) at different depths as well as two basal shear surfaces (BSS I and BSS II) at different stratigraphic depths. One key question is whether the Agadir Slide resulted from a single-phase event or from multi-stage failures. To better understand Agadir Slide emplacement processes, the following key observations need to be taken into account:

(a) The Central slide fairway cuts to the Western slide fairway and the BSS II is deeper than BBS I (Figs. 5a and b). The western boundary (sidewall scarp) of the Central slide fairway is quite steep (up to 18°) (Fig. 3b).

(b) Seismic records indicate that later deposits from the upper headwall area did not bury the lower headwall area (Fig. 5a).

We propose three possible scenarios or hypotheses to investigate Agadir Slide emplacement processes here.

The age model established in this study reveals that the Agadir Slide has an age of 142 ± 1 ka. The first scenario we consider is that the Agadir Slide may have formed from a single-phase event but occurred along two basal shear surfaces (glide planes). Several previous studies have revealed that multiple mass wasting events can be triggered simultaneously and amalgamate or erode each other (Moscardelli et al., 2006; Li et al., 2017). If this was the case for the Agadir Slide, the upper and lower headwall areas would have been generated simultaneously. Mobilized slide deposits along the BSS I in the Western slide fairway would have, then, affected or covered the western boundary (sidewall scarp) of the Central slide fairway. However, as mentioned in observation (a) above, the western sidewall scarp in the Central slide fairway is quite steep and there is no clear evidence from the seismic record that slide deposits from the Western slide fairway covered or buried the sidewall scarp (Fig. 5b). This leads to one conclusion that the Agadir Slide was not generated by one single-phase event, which produced two headwall areas simultaneously.

Several case studies have documented that submarine landslides developed retrogressively in multiple slope failure episodes, e.g., the Hinlopen Slide (Vanneste et al., 2006), the Mauritania Slide Complex (Antobreh and Krastel, 2007), the Storegga Slide (Haflidason et al., 2004) and the Sahara

Slide (Li et al., 2017). If we assume that the Agadir Slide occurred in two retrogressive slide phases, the first slide event would have been triggered in the lower headwall area along the BSS II, followed by the transportation of slide deposits downslope into the Central slide fairway eventually entering into the Agadir Canyon. The second slide event would have been triggered in the upper headwall area retrogressively along the BSS I and the lower headwall area would have been at least partly buried by slide deposits from the upper headwall area. However, this is inconsistent with observation (b) mentioned above. Thus, we suggest that the Agadir Slide did not occur in two phases retrogressively.

The third hypothesis on the emplacement of the Agadir Slide postulates that the Agadir Slide occurred in two slide events at 142 ± 1 ka, although the exact time interval (<2 ka) between these two phases is difficult to determine. The first slide event was triggered in the upper headwall area, which generated pronounced sidewall scarps (Fig. 10a). Approximately 36 km^3 of seafloor sediment was mobilized, leading to almost complete sediment evacuation in the headwall area. The mobilized sediment was transported downslope and several seamounts confined the deposition (e.g., SM1 to SM4). Most slide deposits were transported between SM 2 and SM 4, and only a minor amount of slide deposits were transported to the west of SM 2 and to the east of SM 4 (Fig. 10a). Slide deposits continued beyond SM 2 and SM 4 and were divided into two parts downslope (Fig. 10a). The slide deposits in the western region were transported into the Western slide fairway and later spread out, leading to the generation of positive topography at the western border of the Western slide fairway (Fig. 10a). The eastern region of slide deposits were further confined when they passed between SM3 and SM4 (Fig. 10a).

The second phase of the Agadir Slide began in the southern region of the Central slide fairway, i.e., between SM3 and SM4 (Fig. 10b and c). Here, we identified a pronounced headwall scarp, with a height of 100 m, in the lower headwall area (Fig. 4b). The latter slide event produced the distinguished sidewall scarps throughout the Central slide fairway by reworking the eastern part of Western slide fairway (Fig. 6b). Slide deposits were further transported downslope and entered the pre-existing fairway in the northern part (Fig. 7a). This led to the formation of pronounced sidewall scarps, which were most likely produced by enhanced erosion before the slide entered the Agadir Canyon (Fig. 10b). The increase of the slope gradient from 0.5 to 1.8°, at the transition between the fairway and Agadir Canyon, likely promoted the further transportation of slide deposits into the Agadir Canyon (Fig. 6b).

5.2. Flow history of the Agadir Slide

Our observations reveal that the Agadir Slide affects an area of approximately 5,500 km^2, displaces a volume of 340 km^3, and has a (run-out) distance of 350 km. The Agadir Slide is a large-scale submarine landslide as its size and volume are larger than nearly 80–90% of all documented submarine landslides (Moscardelli and Wood, 2015). Moscardelli and Wood (2008) proposed that different sediment sources, i.e., localized and extrabasinal sources, contributed to the volume of submarine landslides.

The main process that contributes to the Agadir Slide's large-volume results from the mobilization of sediments along the two basal shear surfaces (glide planes) in the headwall areas and the Central and Western slide fairways. This extrabasinal sediment source may relate to variable sediment input from multiple minor slide events generated near the Agadir Slide's source area (Fig. 3a). These slide events may have generated additional sediment that were later transported into the Western and Central slide fairway and Agadir Canyon (Fig. 3a). In addition, salt diapirs are widespread throughout the Agadir Slide area and have played a vital role in shaping the morphology and evolution of the Agadir Slide. Strong erosional processes occurred along the flanks of the salt diapirs, which may enable the addition of material to the slide via collapsing salt diapir flanks. The erosional remnants that separate the BSS I and BSS II could have formed from the presence of salt diapirs that diverted the Agadir Slide (Fig. 6a). These erosional remnants are similar to the "erosional shadow remnants" at the base of the shallowest mass-transport complex along the offshore region of Trinidad (Moscardelli et al., 2006). The presence of erosional remnants indicates the magnitude of the Agadir Slide's large-scale lateral erosive energy when passing the morphological expressions of salt diapirs on the seafloor. These morphological expressions of the salt diapirs acted as physiographic barriers preventing areas of older sea floor from being eroded by passing mass-transport flows (Moscardelli et al., 2006).

High-resolution imaging of the internal architecture of the Agadir Slide allows the investigation of flow behavior during emplacement processes. Close interactions between submarine landslides and the sea floor can lead to the extensive remobilization of pre-existing deposits on the sea bed (Watt et al., 2012; Alves et al., 2014). Debris flows that initiate widespread erosion of subsurface sediments that leads to an increase in the flow volume are capable of creating a basal layer upon which overlying gravity flows can move over long distances (Masson et al., 2006). However, based on our observations, the BBS I and BBS II are roughly parallel to stratification and appear to correlate with the same stratigraphic level (Figs. 5 and 6). The zoomed section of seismic records shows no evidence that the basal shear surfaces remove a large portion of the underlying sediments. Thus, we propose that the flows, associated with slide deposition, are plastic, and do not erode the substratum. The first slide event that occurred in the upper headwall area did not transform into a debris flow, only occurring as a slide along the BSS I. The second event was also a slide and moved downslope along the BSS II. This slide did not evolve into a debris flow at least before entering the Agadir Canyon.

Submarine landslides commonly disintegrate into slide blocks of variable sizes in their toe regions (Alves, 2015). However, few slide blocks are observed in the bathymetric imaging data of the Agadir Slide (Fig. 3a). In reality, not all submarine landslides transform into long run-out turbidity currents. The Sahara Slide occurred as a relatively slow-moving slab-type failure on a low-angle slope. It is likely the elevated cohesiveness of the fine-grained headwall sediments prevented it from disintegrating into turbidity currents (Georgiopoulou et al., 2010). The emplacement of the Agadir Slide may be similar to that of the Sahara Slide. An amount of sufficient kinetic energy was not available initiate the transition into a turbidity current, and erosion at the sidewalls of the slide may have extracted a significant amount of energy out of the system causing the entire slide to slow down. The orientation of small-scale faults identified in the toe region of the Central slide fairway is parallel to the sliding direction and they were produced due to shearing as the slide moved downslope (Fig.

6c), which provides further evidence of slide slow down.

In summary, the sediment transported by the Agadir Slide was: a) almost entirely trapped in the slide fairway and Agadir Canyon and b) was not fast enough along the continental slope to disintegrate and form a turbidity current. Therefore, turbidites from the Moroccan Turbidite System must have another source. No other major landslide scars have been identified in the Agadir Canyon Region. This leaves the Agadir Canyon's head region as the most likely source for turbidites in the Moroccan Turbidite System despite the fact that we observe only small failure scars (<5 km^3) in the head region of the canyon.

5.3. Could the Agadir Slide be the source of turbidite events in the Moroccan Turbidite System?

Submarine landslides and debris flows may transform to turbidity currents on both active and passive continental margins (Wynn et al., 2002; Trofimovs et al., 2008; Clare et al., 2014). Some large-volume submarine landslides (i.e., >100 km^3 of sediment) can rapidly disintegrate into far-reaching turbidity currents along very gentle slopes (Talling et al., 2007b). Flow transformation from a debris flow to a turbidity current has been reported, for instance, during the 1929 Grand Banks submarine landslide (Piper et al., 1999). The Moroccan Turbidite System has hosted numerous landslide-triggered turbidity currents over the past 200 ka (Wynn et al., 2002; Talling et al., 2007a; Hunt et al., 2013a). Most of these turbidity currents derive from the Moroccan margin and were transported into the Moroccan Turbidite System via the Agadir Canyon (e.g., AB5, AB7, and AB12).

The Agadir Slide was the first large-scale submarine landslide to be identified in close vicinity to the Agadir Canyon (Krastel et al., 2016). So, could the Agadir Slide be the source area of one of the turbidite events in the Moroccan Turbidite System? Several lines of evidences have been proposed to assess the relationship between the Agadir Slide and the turbidite events recorded in the Moroccan Turbidite System. Results from magnetic susceptibility stratigraphy provide an age of 142 ± 1 ka for the Agadir Slide, which is older than the nearest turbidite, AB13, by 7 ky. Even assuming a conservative error of 5 kyr (c.f., Urlaub et al., 2013) for AB13, i.e., 140 ka, the Agadir Slide occurred significantly below the 140 ka horizon (Fig. 9b). Therefore, the Agadir Slide is older than 140 ka and does not correlate with any turbidites found down slope in the Moroccan Turbidite System. This indicates that the Agadir Slide was not a turbidite source in the Moroccan Turbidite System.

Most turbidites that originate from the Moroccan margin and fill the intraslope basin mainly occurred during sea-level fall and lowstand stages (Urlaub et al., 2013). The Agadir Slide took place at 142 ± 1 ka during a sea-level lowstand stage. Urlaub et al. (2013) proposed that there is no relationship between the occurrence of submarine landslides and sea-level variations based on a data set of ages for 68 large-volume submarine landslides. Therefore, it is difficult to determine if sea-level variation was one of the controlling factors for Agadir Slide initiation. When considering the presence of two basal shear surfaces (glide planes) in the Agadir Slide, we propose that the preconditioning factor for the Agadir Slide is the presence of these two weak layers. Seismicity related to fault activity and halokinesis are plausible triggers for Agadir Slide initiation. Similar cases have been documented in the Gulf of Mexico, where the occurrence of salt deformation and submarine landslides are also pervasive (Beaubouef and Abreu, 2010). Earthquakes related to salt deformation may play a critical role in initiating slope failures (e.g. Justin and Brandon, 2010; Urgeles and Camerlenghi, 2013).

6. Conclusions

High-resolution multibeam bathymetry data, 2D seismic profiles, and gravity cores have allowed us to investigate the morphology, internal character, and origin of the Agadir Slide on the NW African margin. The main conclusions of this study are:

(1) The Agadir Slide affected an area of 5,500 km^2, displaced a volume of 340 km^3, and shows a (run-out) distance of 350 km. The Agadir Slide includes two headwall areas, the Western slide fairway and Central slide fairway.

(2) The volume calculations reveal that most Agadir Slide deposits, approximately 170 km^3, accumulated in the Central and Western slide fairways, while approximately 70 km^3 of slide deposits were trapped in the Agadir Canyon.

(3) The Agadir Slide was emplaced at 142 ka in two main phases. The first phase of the Agadir

Slide was triggered in the upper headwall area and the second phase occurred in the lower headwall area. It is likely the presence of two weak layers preconditioned the Agadir Slide, and seismicity associated with fault activity and halokinesis are the main triggers of the Agadir Slide.

(4) Salt structures affecting the seafloor have played a vital role on the distribution and evolution of the Agadir Slide. The slide does not correlate with turbidites down slope in the Moroccan Turbidite System. Therefore, we suggest that the Agadir Slide traveled relatively slowly and did not disintegrate into a fluid turbidity current. The turbidite source in the Moroccan Turbidite System is, therefore, likely to be at the head of the Agadir Canyon.

The detailed investigation of the Agadir Slide on the NW African margin reveals that not all submarine landslides transform into turbidity currents. This is an important case-study to better understand the flow behavior of submarine landslides on other continental margins. It is also essential to assess the hazards and risks of submarine landslides by integrating multi-disciplinary approaches.

Acknowledgments

We thank the crews and captains of RV Maria S. Merian Cruise MSM32. Financial support was provided by the Deutsche Forschungsgemeinschaft (DFG). Dr. Wei Li is funded by CAS Pioneer Hundred Talents Program. The paper benefited from the constructive comments of the Editor Prof. Peter Shearer, Dr. Lorena Moscardelli and one anonymous reviewer.

References

Alves, T.M., 2015. Submarine slide blocks and associated soft-sediment deformation in deep-water basins: A review. Marine and Petroleum Geology 67, 262-285.

Alves, T.M., Cartwright, J., 2009. Volume balance of a submarine landslide in the Espirito Santo Basin, offshore Brazil: Quantifying seafloor erosion, sediment accumulation and depletion. Earth and Planetary Science Letters 288, 572-580.

Alves, T.M., Strasser, M., Moore, G.F., 2014. Erosional features as indicators of thrust fault activity (Nankai Trough, Japan). Marine Geology 356, 5-18.

Antobreh, A.A., Krastel, S., 2007. Mauritania Slide Complex: morphology, seismic characterisation and processes of formation. International Journal of Earth Sciences 96, 451-472.

Baeten, N.J., Laberg, J.S., Vanneste, M., Forsberg, C.F., Kvalstad, T.J., Forwick, M., Vorren, T.O., Haflidason, H.,

2014. Origin of shallow submarine mass movements and their glide planesdsedimentological and geotechnical analyses from the continental slope off northern Norway. Journal of Geophysical Research: Earth Surface 119.

Beaubouef, R.T., Abreu, V., 2010. MTCs of the Brazos-Trinity Slope System; Thoughts on the Sequence Stratigraphy of MTCs and Their Possible Roles in Shaping Hydrocarbon Traps, in: Mosher, D.C., Shipp, R.C., Moscardelli, L., Chaytor, J.D., Baxter, C.D.P., Lee, H.J., Urgeles, R. (Eds.), Submarine Mass Movements and Their Consequences. Springer Netherlands, Dordrecht, pp. 475-490.

Clare, M.A., Talling, P.J., Challenor, P., Malgesini, G., Hunt, J., 2014. Distal turbidites reveal a common distribution for large (>0.1 km3) submarine landslide recurrence. Geology 42, 263-266.

Dunlap, D.B., Wood, L.J., Weisenberger, C., Jabour, H., 2010. Seismic geomorphology of offshore Morocco's east margin, Safi Haute Mer area. AAPG Bulletin 94, 615-642.

Frenz, M., Wynn, R.B., Georgiopoulou, A., Bender, V.B., Hough, G., Masson, D.G., Talling, P.J., Cronin, B.T., 2009. Provenance and pathways of late Quaternary turbidites in the deep-water Agadir Basin, northwest African margin. International Journal of Earth Sciences 98, 721-733.

Freudenthal, T., Meggers, H., Henderiks, J., Kuhlmann, H., Moreno, A., Wefer, G., 2002. Upwelling intensity and filament activity off Morocco during the last 250,000 years. Deep Sea Research Part II: Topical Studies in Oceanography 49, 3655-3674.

Gamboa, D., Alves, T., Cartwright, J., Terrinha, P., 2010. MTD distribution on a 'passive' continental margin: The Espírito Santo Basin (SE Brazil) during the Palaeogene. Marine and Petroleum Geology 27, 1311-1324.

Gee, M.J.R., Masson, D.G., Watts, A.B., Allen, P.A., 1999. The Saharan debris flow: an insight into the mechanics of long runout submarine debris flows. Sedimentology 46, 317-335.

Georgiopoulou, A., Masson, D.G., Wynn, R.B., Krastel, S., 2010. Sahara Slide: Age, initiation, and processes of a giant submarine slide. Geochemistry, Geophysics, Geosystems 11, 1-22.

Haflidason, H., Sejrup, H.P., Nygård, A., Mienert, J., Bryn, P., Lien, R., Forsberg, C.F., Berg, K., Masson, D., 2004. The Storegga Slide: architecture, geometry and slide development. Marine Geology 213, 201-234.

Hampton, M.A., Lee, H.J., Locat, J., 1996. Submarine landslides. Reviews of Geophysics 34, 33-59.

Hühnerbach, V., Masson, D.G., 2004. Landslides in the North Atlantic and its adjacent seas: an analysis of their morphology, setting and behaviour. Marine Geology 213, 343-362.

Hunt, J.E., Wynn, R.B., Talling, P.J., Masson, D.G., 2013a. Frequency and timing of landslide-triggered turbidity currents within the Agadir Basin, offshore NW Africa: Are there associations with climate change, sea level change and slope sedimentation rates? Marine Geology 346, 274-291.

Hunt, J.E., Wynn, R.B., Talling, P.J., Masson, D.G., 2013b. Turbidite record of frequency and source of large volume (>100 km3) Canary Island landslides in the last 1.5 Ma: Implications for landslide triggers and geohazards. Geochemistry, Geophysics, Geosystems 14, 2100-2123.

Justin, S., Brandon, D., 2010. Overpressure and earthquake initiated slope failure in the Ursa region, northern Gulf of Mexico. Journal of Geophysical Research: Solid Earth 115.

Krastel, S., Behmann, J.-H., Völker, D., Stipp, M., Berndt, C., Urgeles, R., Chaytor, J., Huhn, K., Strasser, M., Harbitz, C.B., 2014. Submarine mass movements and their consequences. 6th International Symposium. Advances in Natural and Technological Research 37, pp 683.

Krastel, S., Wynn, R.B., Georgiopoulou, A., Geersen, J., Henrich, R., Meyer, M., Schwenk, T., 2012. Large-Scale Mass Wasting on the Northwest African Continental Margin: Some General Implications for Mass Wasting on Passive Continental Margins. 189-199.

Krastel, S., Wynn, R.B., Feldens, P., Schürer, A., Böttner, C., Stevenson, C., Cartigny, M.J.B., Hühnerbach, V., Unverricht, D., 2016. Flow Behaviour of a Giant Landslide and Debris Flow Entering Agadir Canyon, NW Africa, in: Lamarche, G., Mountjoy, J., Bull, S., Hubble, T., Krastel, S., Lane, E., Micallef, A., Moscardelli, L., Mueller, C., Pecher, I., Woelz, S. (Eds.), Submarine Mass Movements and their Consequences: 7th International Symposium. Springer International Publishing, Cham, pp. 145-154.

Kuhlmann, H., Freudenthal, T., Helmke, P., Meggers, H., 2004. Reconstruction of paleoceanography off NW Africa during the last 40,000 years: influence of local and regional factors on sediment accumulation. Marine Geology 207, 209-224.

Li, W., Alves, T.M., Urlaub, M., Georgiopoulou, A., Klaucke, I., Wynn, R.B., Gross, F., Meyer, M., Repschläger, J., Berndt, C., Krastel, S., 2017. Morphology, age and sediment dynamics of the upper headwall of the Sahara Slide Complex, Northwest Africa: Evidence for a large Late Holocene failure. Marine Geology 393, 109-123.

Masson, D.G., 1994. Late Quaternary turbidity current pathways to the Madeira Abyssal Plain and some constraints on turbidity current mechanisms. Basin Research 6, 17-33.

Masson, D.G., Harbitz, C.B., Wynn, R.B., Pedersen, G., Løvholt, F., 2006. Submarine landslides: processes, triggers and hazard prediction. Philosophical Transactions of the Royal Society A: Mathematical, Physical and Engineering Sciences 364, 2009-2039.

Moscardelli, L., Wood, L., 2008. New classification system for mass transport complexes in offshore Trinidad. Basin Research 20, 73-98.

Moscardelli, L., Wood, L., 2015. Morphometry of mass-transport deposits as a predictive tool. GSA Bulletin 128

(1-2): 47-80.
Moscardelli, L., Wood, L., Mann, P., 2006. Mass-transport complexes and associated processesin the offshore area of Trinidad and Venezuela. AAPG Bulletin 90, 1059-1088.
Mosher, D.C., Moscardelli, L., Shipp, R.C., Chaytor, J.D., Baxter, C.D.P., Lee, H.J., Urgeles, R., 2010. Submarine Mass Movements and Their Consequences, in: Mosher, D.C., Shipp, R.C., Moscardelli, L., Chaytor, J.D., Baxter, C.D.P., Lee, H.J., Urgeles, R. (Eds.), Submarine Mass Movements and Their Consequences. Springer Netherlands, Dordrecht, pp. 1-8.
Piper, D.J.W., Cochonat, P., Morrison, M.L., 1999. The sequence of events around the epicentre of the 1929 Grand Banks earthquake: initiation of debris flows and turbidity current inferred from sidescan sonar. Sedimentology 46, 79-97.
Seibold, E., 1982, The northwest African continental margin-An introduction, in U. Von Rad, K. Hinz, M. Sarnthein, and E. Seibold, eds., Geology of the northwest African continental margin: Berlin, Springer-Verlag, p. 215-269.
Smith, W.H.F., Wessel, P., 1990. Gridding with continuous curvature splines in tension. Geophysics 55, 293-305.
Stevenson, C.J, Talling, P.J., Wynn, R.B., Masson, D.G., Hunt, J.E., Frenz, M., Akhmetzhanhov, A., and Cronin, B.T., 2013, The flows that left no trace: Very large-volume turbidity currents that bypassed sediment through submarine channels without eroding the sea floor: Marine and Petroleum Geology 41, 186-205.
Stevenson, C.J., Talling, P.J., Masson, D.G., Sumner, E.J., Frenz, M., and Wynn, R.B., 2014. The spatial and temporal distribution of grain-size breaks in turbidites. Sedimentology 61, 1120-1156.
Talling, P.J., Amy, L.A., Wynn, R.B., 2007a. New insight into the evolution of large-volume turbidity currents: comparison of turbidite shape and previous modelling results. Sedimentology 54, 737-769.
Talling, P.J., Wynn, R.B., Masson, D.G., Frenz, M., Cronin, B.T., Schiebel, R., Akhmetzhanov, A.M., Dallmeier-Tiessen, S., Benetti, S., Weaver, P.P., Georgiopoulou, A., Zuhlsdorff, C., Amy, L.A., 2007b. Onset of submarine debris flow deposition far from original giant landslide. Nature 450, 541-544.
Tappin, D.R., Grilli, S.T., Harris, J.C., Geller, R.J., Masterlark, T., Kirby, J.T., Shi, F., Ma, G., Thingbaijam, K.K.S., Mai, P.M., 2014. Did a submarine landslide contribute to the 2011 Tohoku tsunami? Marine Geology 357, 344-361.
Tari, G., Jabour, H., 2013. Salt tectonics along the Atlantic margin of Morocco. Geological Society, London, Special Publications 369, 337-353.
ten Brink, U.S., Geist, E.L., Andrews, B.D., 2006. Size distribution of submarine landslides and its implication to

tsunami hazard in Puerto Rico. Geophysical Research Letters 33, L11307.

Thomson, J., Weaver, P.P.E., 1994. An AMS radiocarbon method to determine the emplacement time of recent deep-sea turbidites. Sedimentary Geology 89, 1-7.

Trofimovs, J., Sparks, R.S.J., Talling, P.J., 2008. Anatomy of a submarine pyroclastic flow and associated turbidity current: July 2003 dome collapse, Soufrière Hills volcano, Montserrat, West Indies. Sedimentology 55, 617-634.

Urgeles, R., Camerlenghi, A., 2013. Submarine landslides of the Mediterranean Sea: trigger mechanisms, dynamics and frequency- magnitude distribution. Journal of Geophysical Research Earth Surface 118, 2600-2618.

Urlaub, M., Talling, P.J., Masson, D.G., 2013. Timing and frequency of large submarine landslides: implications for understanding triggers and future geohazard. Quaternary Science Reviews 72, 63-82.

Vanneste, M., Mienert, J., Bunz, S., 2006. The Hinlopen Slide: A giant, submarine slope failure on the northern Svalbard margin, Arctic Ocean. Earth and Planetary Science Letters 245, 373-388.

Watt, S.F.L., Talling, P.J., Vardy, M.E., Heller, V., Hühnerbach, V., Urlaub, M., Sarkar, S., Masson, D.G., Henstock, T.J., Minshull, T.A., Paulatto, M., Le Friant, A., Lebas, E., Berndt, C., Crutchley, G.J., Karstens, J., Stinton, A.J., Maeno, F., 2012. Combinations of volcanic-flank and seafloor-sediment failure offshore Montserrat, and their implications for tsunami generation. Earth and Planetary Science Letters 319-320, 228-240.

Wefer, G. and cruise participants, 1997. Report and preliminary results of METEOR-Cruise M37/1, Lisbon-Las Palmas, 4.12.-23.12.1996. Berichte aus dem Fachbereich Geowissenschaften der Universität Bremen, 090. Department of Geosciences, Bremen University.

Wynn, R.B., Masson, D.G., Stow, D.A.V., Weaver, P.P.E., 2000. The Northwest African slope apron: a modern analogue for deep-water systems with complex seafloor topography. Marine and Petroleum Geology 17, 253-265.

Wynn R.B., Talling P.J., Masson D.G., Stevenson C.J., Cronin B.T., Bas T.P.L., 2010. Investigating the Timing, Processes and Deposits of One of the World's Largest Submarine Gravity Flows: The 'Bed 5 Event' Off Northwest Africa. In: Mosher D.C. et al. (eds) Submarine Mass Movements and Their Consequences. Advances in Natural and Technological Hazards Research, vol 28. Springer, Dordrecht.

Wynn, R.B., Weaver, P.P.E., Masson, D.G., Stow, D.A.V., 2002. Turbidite depositional architecture across three interconnected deep-water basins on the north-west African margin. Sedimentology 49, 669-695.

Figure Captions

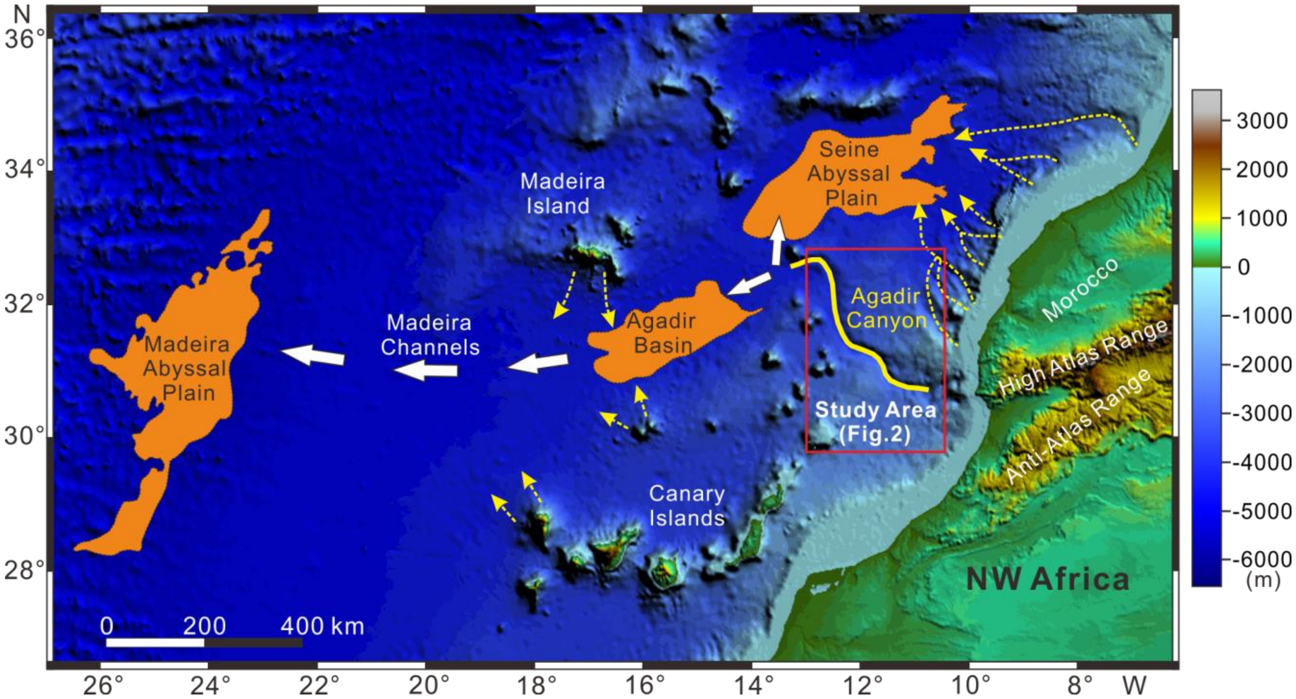

Figure 1. Combined bathymetric and topographic map showing key geomorphological features offshore of the Northwest African continental margin (e.g., the Canary Islands, Madeira Island, High Atlas Range, and Anti-Atlas Range). The red box highlights the location of the study area. The yellow solid line indicates the course of the Agadir Canyon (Wynn et al., 2000). The Moroccan Turbidite System extends through three interconnected basins, marked in orange on the figure: the Seine Abyssal Plain, the Agadir Basin, and the Madeira Abyssal Plain. The yellow dashed lines indicate the principal turbidity current transport directions that enter into the Morocco Turbidite System (modified after Wynn et al., 2002).

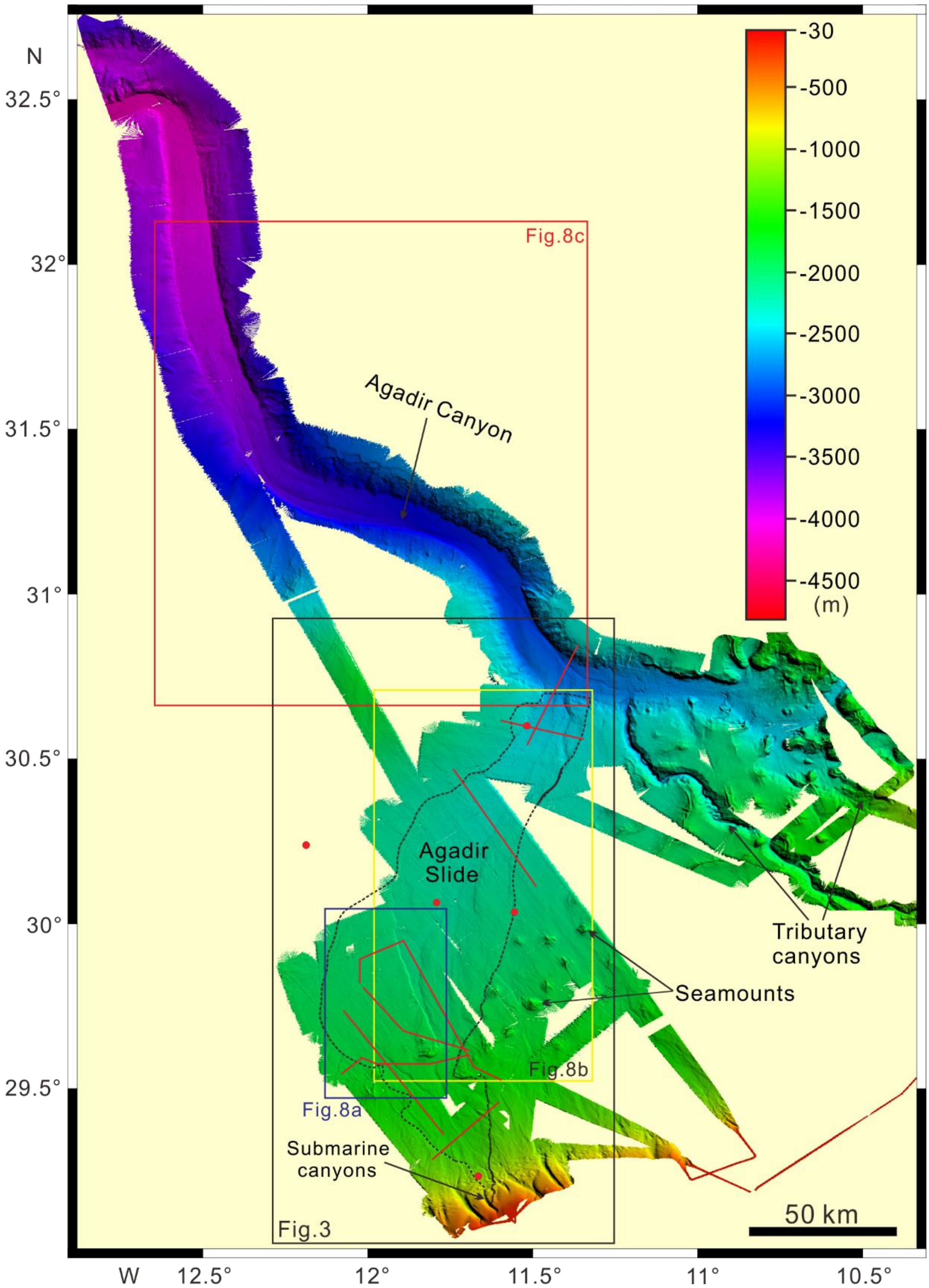

Figure 2. Multibeam bathymetric map of the study area illustrating the distribution and seafloor morphology of the Agadir Canyon and the Agadir Slide. Several tributary canyons are identified at the headwall of the Agadir Canyon. The boxes with different colors represent the figure locations used in the following sections of this study. The black dashed line indicates the boundary of the Agadir Slide.

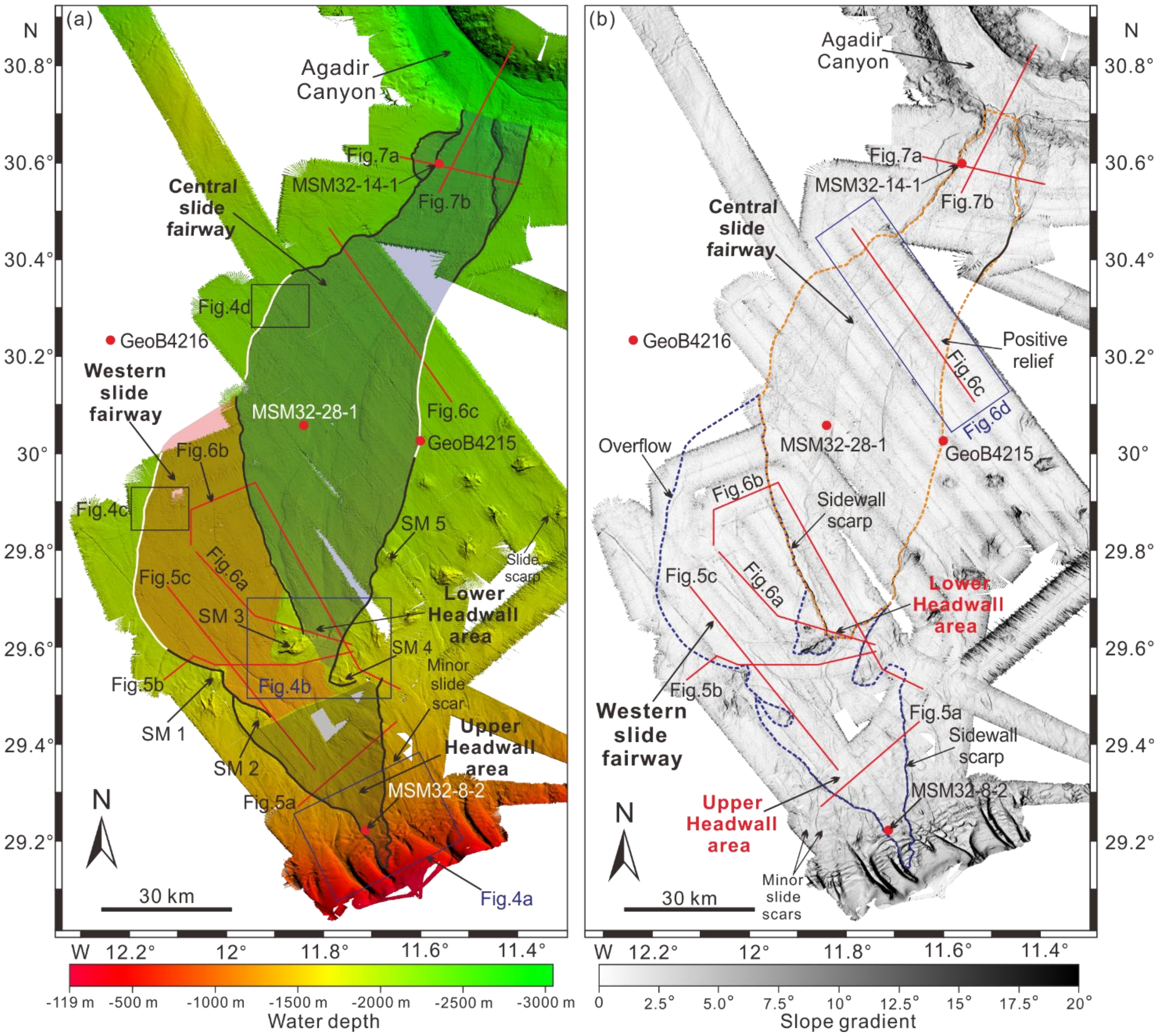

Figure 3. (a) High-resolution multibeam bathymetric map showing a detailed view of the seafloor morphology of the Agadir Slide. The red solid lines indicate the locations of 2D seismic data presented in this study. Five major seamounts are also marked in the figure. The black solid lines indicate the escarpment of the Agadir Slide. The white solid lines represent regions of positive reliefs. (b) Slope gradient map of the Agadir Slide area revealing two pronounced headwall areas and their associated sidewall scarps. The red circles represent the location of the gravity cores described in this study. The purple and orange dashed lines indicate the distribution of the BSS I and BSS II, respectively.

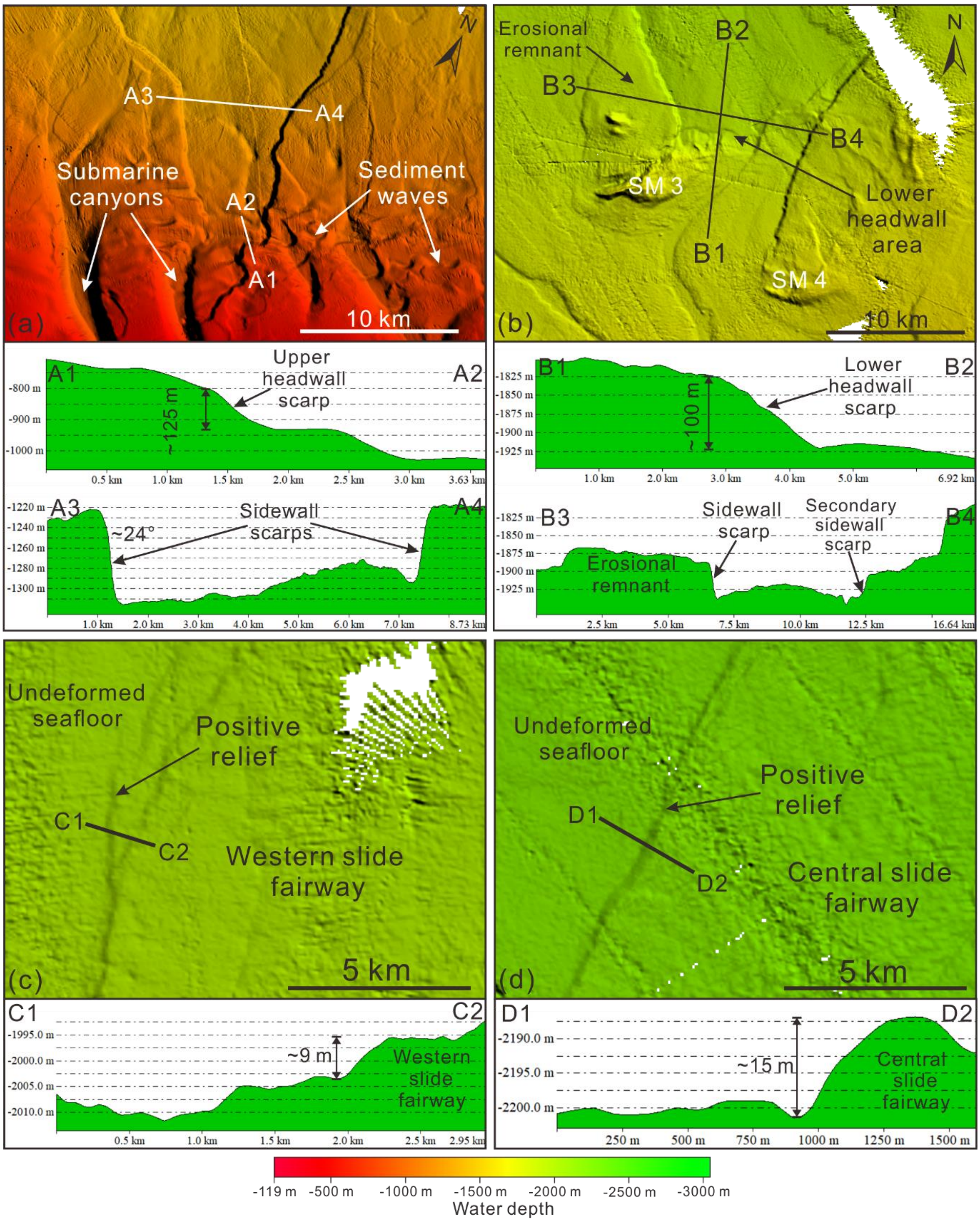

Figure 4. (a) Multibeam bathymetric map showing the detailed seafloor morphology of the upper headwall area. Submarine canyons and a field of sediment waves are observed in the upslope area. The headwall and sidewall scarps in the upper headwall area are illustrated on the topographical profiles of A1–A2 and A3–A4, respectively. (b) Detailed geomorphology of the lower headwall area showing the seamounts (SM 3 and 4) and an erosional remnant in the downslope region of SM 3. Topographical profiles B1–B2 and B3–B4 reveal the headwall and sidewall scarps in the lower

headwall area. (c) Positive relief imaged in the Western slide fairway on the bathymetrical map that exhibits a height difference of approximately 9 m on the C1–C2 topographical profile. (d) Multibeam bathymetric map showing positive relief in the Central slide fairway with a height difference of approximately 15 m on the D1–D2 topographical profile. Refer to the bathymetric map locations in Fig. 3a.

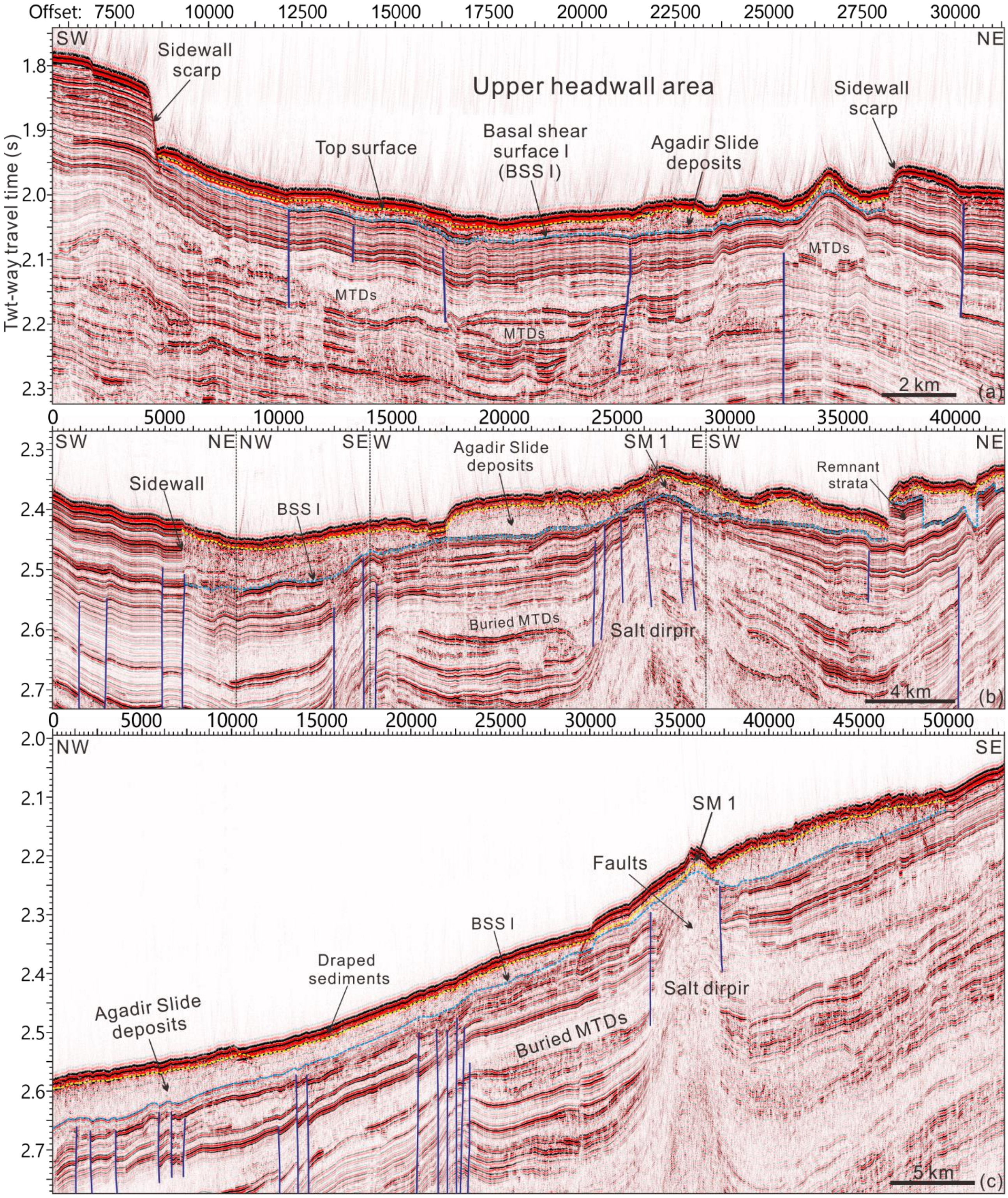

Figure 5. (a) Two-dimensional (2D) seismic profile across the headwall area of the Agadir Slide showing sidewall scarps and multiple mass-transport deposits (MTDs). The blue and yellow dashed lines indicate the base and top surfaces of the Agadir Slide, respectively. Note that the slide deposits in the headwall area are very thin due to the almost entire evacuation of this region. (b) Two-dimensional (2D) seismic profile traversing the Western and Central slide fairways from west to east.

The profile highlights the relatively thick Agadir Slide deposits and the presence of a developed salt diapir underneath the Agadir Slide. (c) Two-dimensional (2D) seismic profile, oriented SE–NW, crossing the upper headwall area and the Western slide fairway. The figure reveals the distinct separation between the various Agadir Slide deposits by salt diapir in parts of the headwall area.

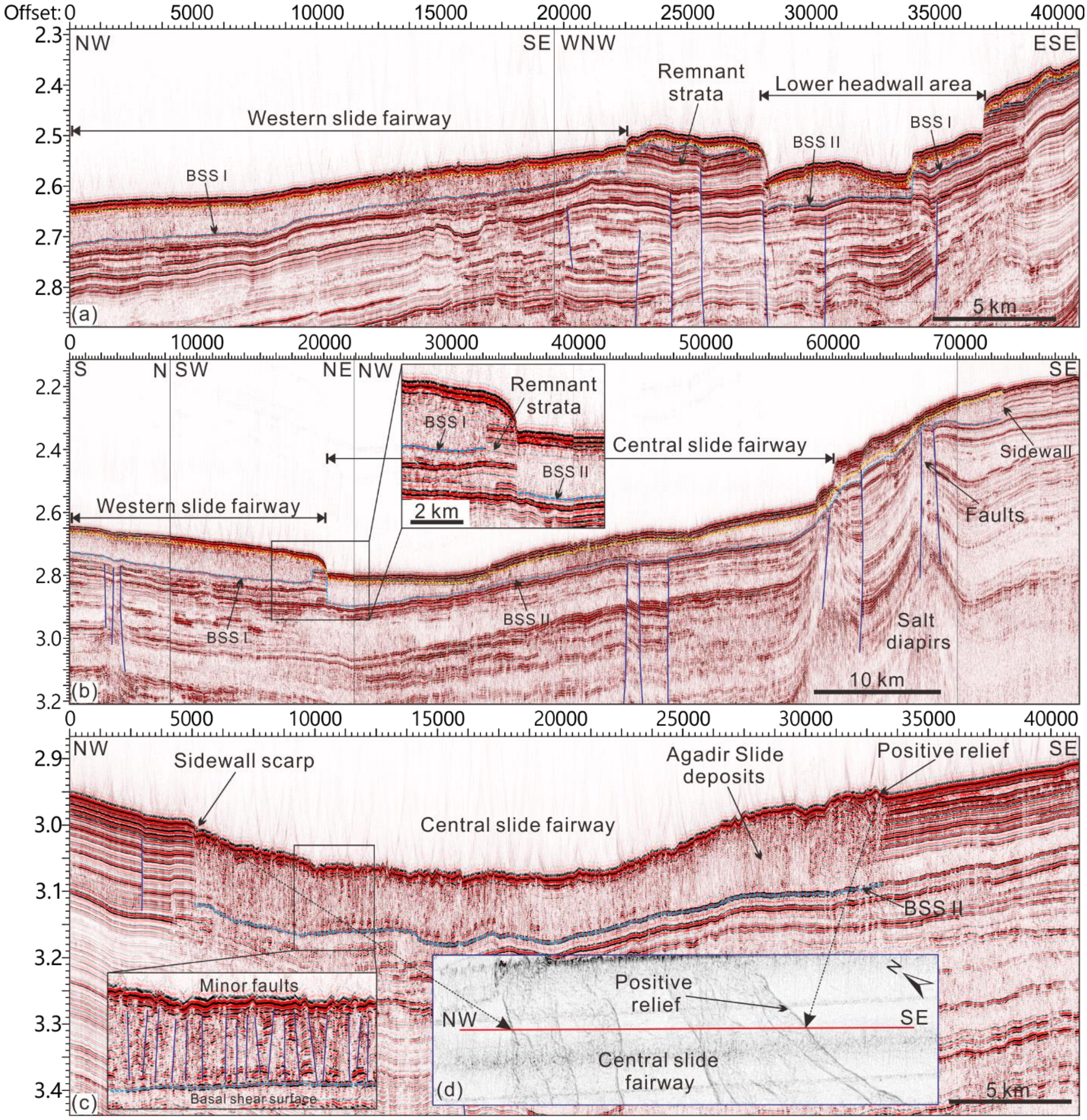

Figure 6. (a) Two-dimensional (2D) seismic profile crossing the Western slide fairway and the Central slide fairway, from northwest to southeast. This seismic profile shows the basal shear surfaces (BSS I and II) of the Agadir Slide rooted at different stratigraphic depths. Note that numerous faults exist below the Agadir Slide deposits. (b) Two-dimensional (2D) seismic profile denoting the presence of thicker slide deposits in the Western slide fairway compared with those in the Central

slide fairway. Note once again the distinct stratigraphic depths of the basal shear surfaces in both areas and the undisturbed strata in-between. (c) Two-dimensional (2D) seismic profile across the Central slide fairway that reveals a sidewall scarp to the northwest and slide deposits with a positive morphology to the southeast. Several buried MTDs are observed underneath the Agadir Slide deposits. (d) Slope gradient map showing positive relief in the toe region of the Central slide fairway (Refer to Fig. 3b for the location).

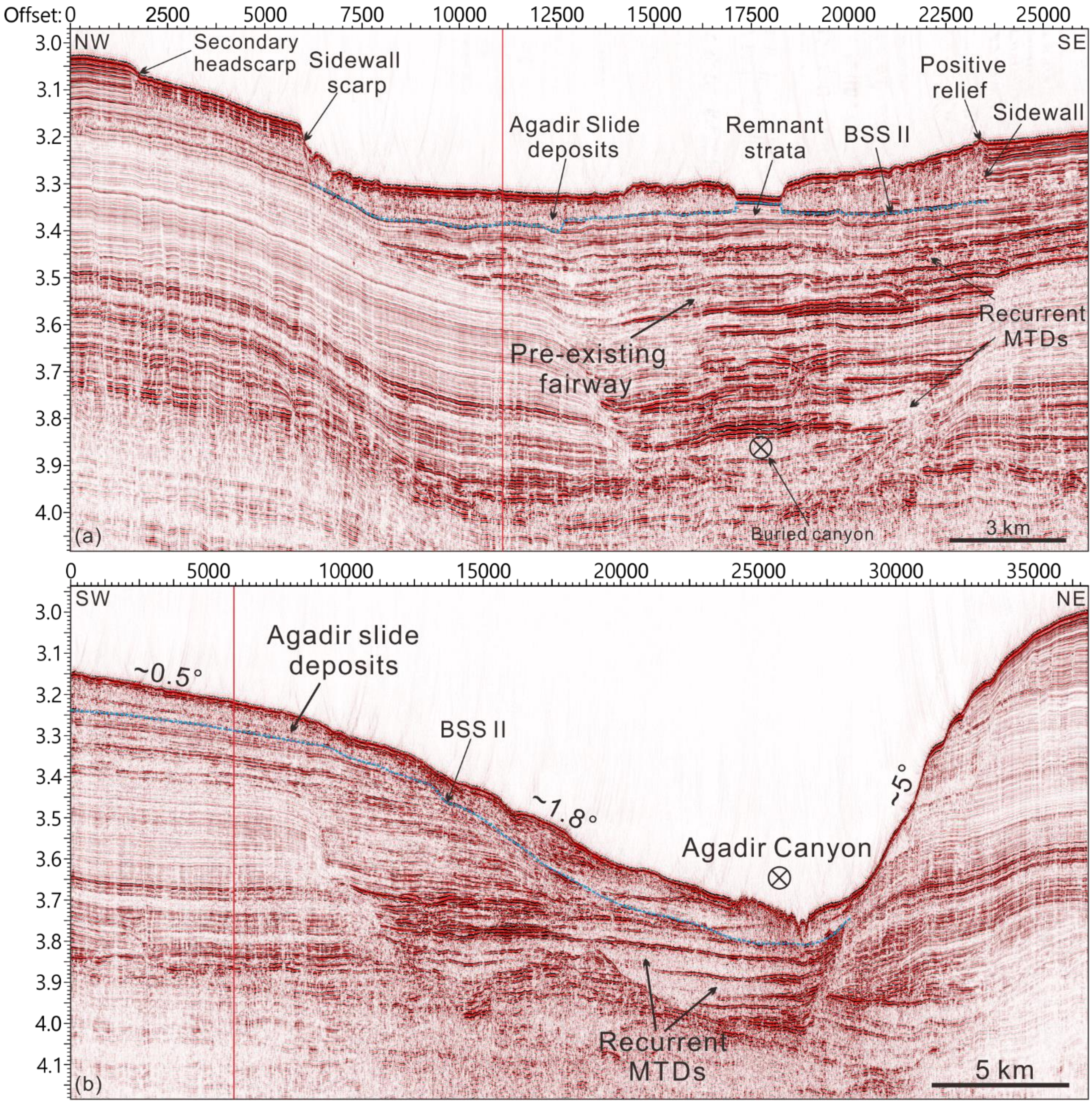

Figure 7. (a) Two-dimensional (2D) seismic profile traversing the southern region of the Central slide fairway. The profile reveals a buried submarine canyon filled by multiple MTDs and a secondary

headwall scarp to the northwest. Note that slide deposits show positive relief compared with the adjacent undisturbed strata. (b) Two-dimensional (2D) seismic profile across the southernmost region of the Central slide fairway. In this location, the Agadir Canyon has multiple stacked MTDs within its interior. The northeastern flank of the Agadir Canyon is much steeper than its southwestern counterpart.

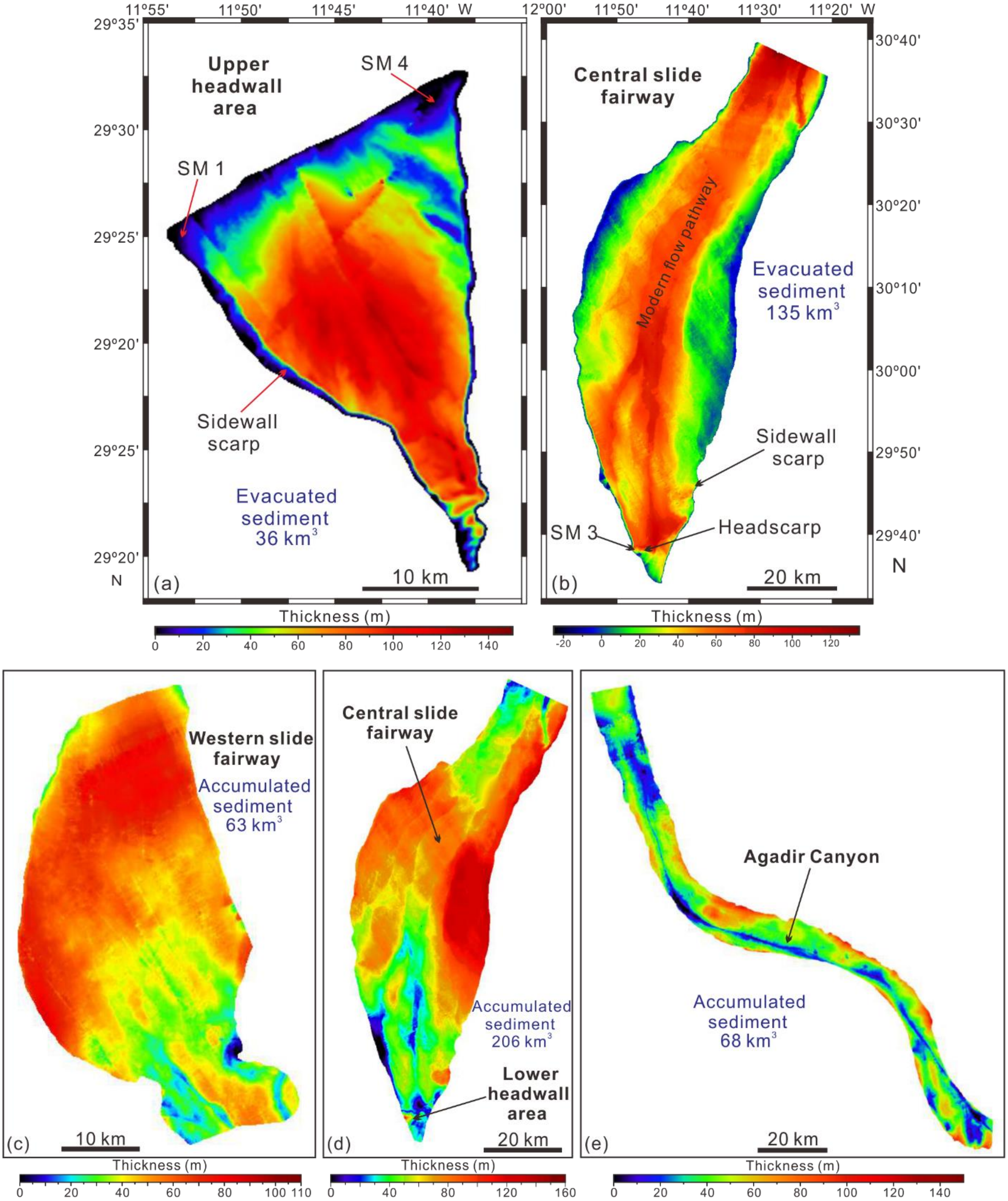

Figure 8. (a) Evacuated sediment thickness map in the headwall that indicates that a total volume of

36 km^3 and a thickness of up to 140 m of sediment were removed from the headwall area. (b) Evacuated (mobilized) sediment thickness map of the Central slide fairway revealing that nearly all sediments were displaced along the Central slide fairway's axis. Negative values at the flanks of the Central slide fairway indicate larger slide deposit accumulation compared with the surrounding unaffected sea floor. (c) Thickness map of slide deposits in the Western slide fairway showing that the majority of slide deposits are located in the northern region of the Western slide fairway. (d) Thickness map of slide deposits in the Central slide fairway revealing a complex sediment distribution. Note that most of the slide deposits in this region are near the eastern and western borders of the Central slide fairway. (e) Thickness map of slide deposits trapped within the Agadir Canyon.

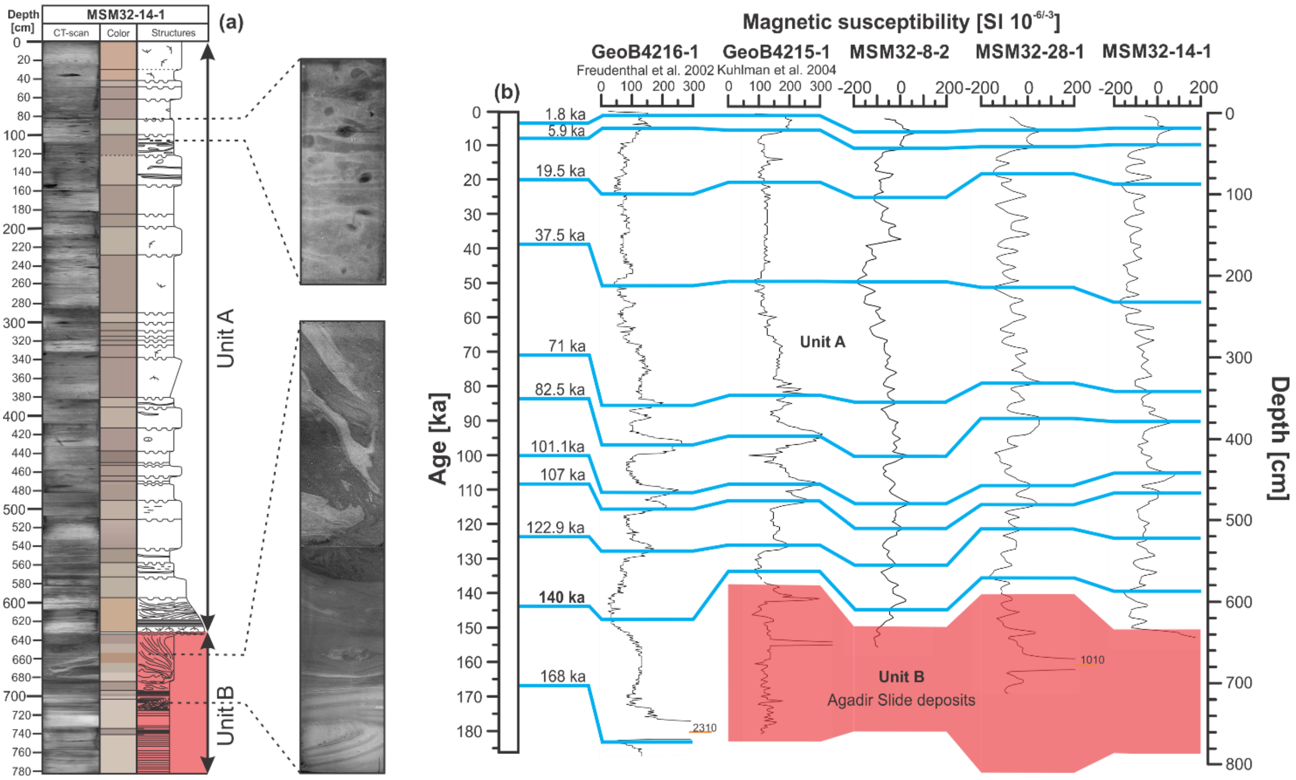

Figure 9. (a) CT-scan and visual description of gravity core MSM32-14-1, which illustrate the color and sedimentary structures. Unit A represents a continuous succession of hemipelagic sediment and Unit B (marked in red) represents the Agadir Slide deposits. The inset displays the remobilized sediment. (b) Sediment-core correlations across the Agadir Slide area. Unit B represents Agadir Slide deposits (marked in red). Blue lines correlate the Magnetic Susceptibility tie-points along the full transect. The respective ages for each tie-point in the GeoB 4216-1 and GeoB 4215-2 cores were

extracted from data sets published in Freudenthal et al. (2002) and Kuhlman et al. (2004).

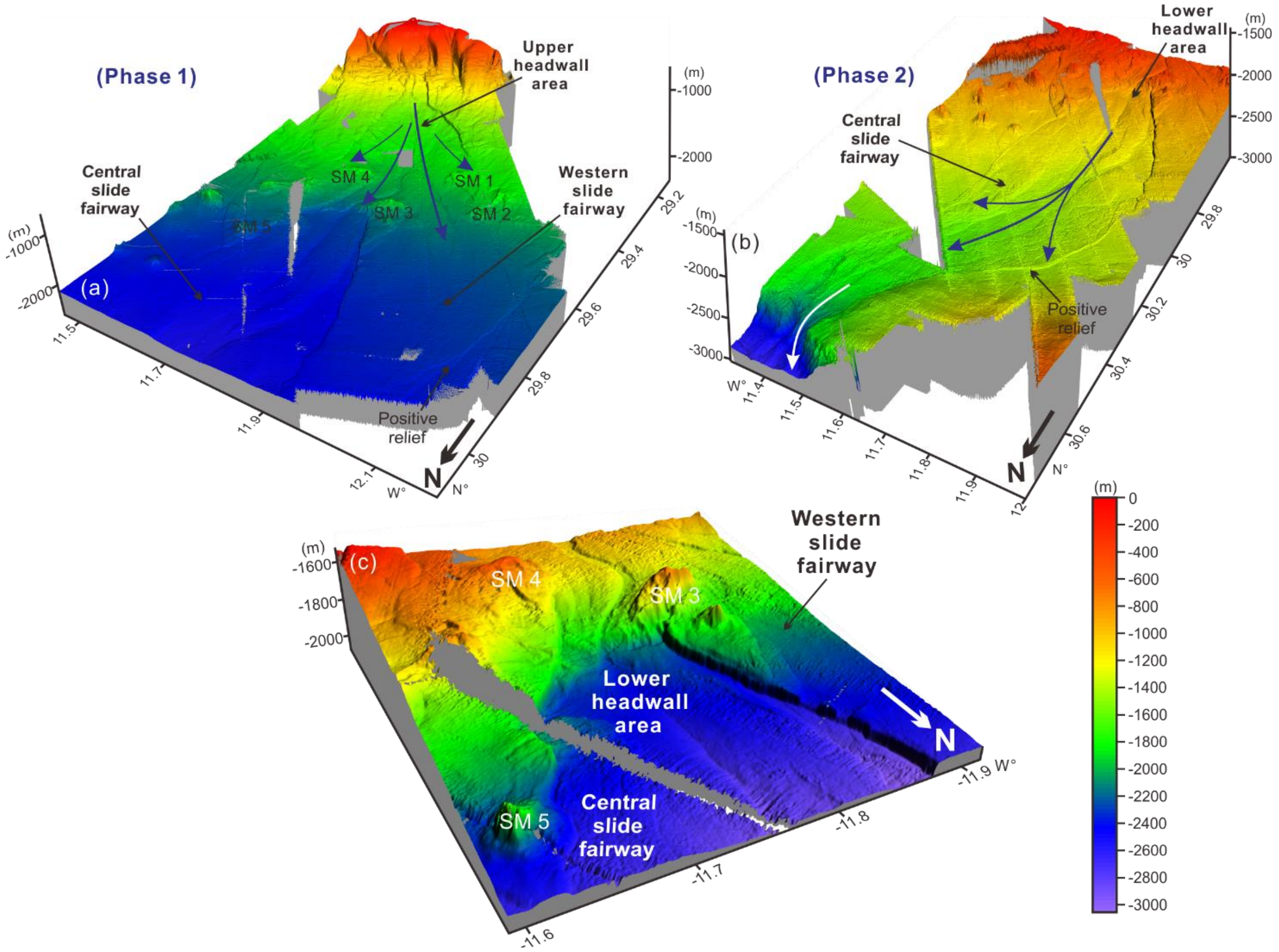

Figure 10. A three-dimensional morphological model illustrating the key emplacement processes occurring in the Agadir Slide. (a) The first phase of the Agadir Slide was triggered in the upper headwall area and slide deposits were diverted by the seamounts. The blue arrows indicate the directions of mass movement. (b) The second phase of the Agadir Slide was triggered in the lower headwall area and slide deposits were transported downslope eventually entering into the Agadir Canyon. (c) 3D bathymetric view of the lower headwall area.